



Get Clarity On Generics

Cost-Effective CT & MRI Contrast Agents

**FRESENIUS
KABI**

WATCH VIDEO

AJNR

This information is current as
of August 5, 2025.

















Assessing Perfusion in Steno-Occlusive Cerebrovascular Disease Using Transient Hypoxia-Induced Deoxyhemoglobin as a Dynamic Susceptibility Contrast Agent

Ece Su Sayin, James Duffin, Vittorio Stumpo, Jacopo Bellomo, Marco Piccirelli, Julien Poublanc, Vepeson Wijeya, Andrea Para, Athina Pangalu, Andrea Bink, Bence Nemeth, Zsolt Kulcsar, David J. Mikulis, Joseph A. Fisher, Olivia Sobczyk and Jorn Fierstra

AJNR Am J Neuroradiol published online 21 December 2023

<http://www.ajnr.org/content/early/2023/12/21/ajnr.A8068>

Assessing Perfusion in Steno-Occlusive Cerebrovascular Disease Using Transient Hypoxia-Induced Deoxyhemoglobin as a Dynamic Susceptibility Contrast Agent

 Ece Su Sayin,  James Duffin,  Vittorio Stumpo,  Jacopo Bellomo,  Marco Piccirelli,  Julien Poulanc,  Vepeson Wijeya,  Andrea Para,  Athina Pangalu,  Andrea Bink,  Bence Nemeth,  Zsolt Kulcsar,  David J. Mikulis,  Joseph A. Fisher,  Olivia Sobczyk, and  Jorn Fierstra



ABSTRACT

BACKGROUND AND PURPOSE: Resting brain tissue perfusion in cerebral steno-occlusive vascular disease can be assessed by MR imaging using gadolinium-based susceptibility contrast agents. Recently, transient hypoxia-induced deoxyhemoglobin has been investigated as a noninvasive MR imaging contrast agent. Here we present a comparison of resting perfusion metrics using transient hypoxia-induced deoxyhemoglobin and gadolinium-based contrast agents in patients with known cerebrovascular steno-occlusive disease.

MATERIALS AND METHODS: Twelve patients with steno-occlusive disease underwent DSC MR imaging using a standard bolus of gadolinium-based contrast agent compared with transient hypoxia-induced deoxyhemoglobin generated in the lungs using an automated gas blender. A conventional multi-slice 2D gradient echo sequence was used to acquire the perfusion data and analyzed using a standard tracer kinetic model. MTT, relative CBF, and relative CBV maps were generated and compared between contrast agents.

RESULTS: The spatial distributions of the perfusion metrics generated with both contrast agents were consistent. Perfusion metrics in GM and WM were not statistically different except for WM MTT.

CONCLUSIONS: Cerebral perfusion metrics generated with noninvasive transient hypoxia-induced changes in deoxyhemoglobin are very similar to those generated using a gadolinium-based contrast agent in patients with cerebrovascular steno-occlusive disease.

ABBREVIATIONS: BOLD = blood oxygen level-dependent; CNR = contrast-to-noise ratio; ΔS = BOLD signal change; dOHb = deoxyhemoglobin; GBCA = gadolinium-based contrast agents; $P_{ET}O_2$ = end-tidal partial pressure of oxygen; PO_2 = partial pressure of oxygen; rCBF = relative CBF; rCBV = relative CBV; THx-dOHb = transient hypoxia-induced deoxyhemoglobin

Angiography can characterize disease-related structural change in major cerebral arteries that can impede blood flow, but it has a limited ability to determine hemodynamic effects at the tissue level.¹ However, DSC MR imaging can measure resting perfusion metrics such as MTT, relative CBF (rCBF), and relative CBV

(rCBV) by tracing the passage of a susceptibility contrast agent through the cerebral vasculature.


Gadolinium-based contrast agents (GBCA) are commonly used because they are strongly paramagnetic and generate robust susceptibility signal changes. Nevertheless, possible long-term risks^{2,3} and measurement inaccuracies^{4,5} when using GBCA indicates the need for new alternative contrast agents.

Consequently, the paramagnetic properties of intrinsically generated changes in deoxyhemoglobin (dOHb)⁶ have recently been explored as an MR imaging contrast agent.^{7,8} Normally, breathing room air oxygenates the mixed venous blood, resulting in fully oxygenated blood returning in the pulmonary veins and into the systemic circulation. Reductions in dOHb in the arteries can be generated by administering a hypoxic inspired gas mixture. In this case, the mixed venous blood fails to fully oxygenate, allowing an increase in dOHb to pass into the arterial blood. Subsequent breathing of a normoxic gas mixture reoxygenates the hemoglobin in subsequent recirculation of the blood. The unsaturated blood generated during transient hypoxia acts as a transient change in

Received July 21, 2023; accepted after revision November 1.

From the Departments of Physiology (E.S.S., J.D., J.A.F.), and Medical Biophysics (D.J.M.), University of Toronto, Toronto, Ontario, Canada; Joint Department of Medical Imaging and the Functional Neuroimaging Lab (E.S.S., J.P., V.W., A. Para, D.J.M., O.S.), University Health Network, Toronto, Ontario, Canada; Department of Anesthesia and Pain Management (J.D., J.A.F.), University Health Network, University of Toronto, Toronto, Ontario, Canada; and Departments of Neurosurgery (V.S., J.B., J.F.) and Neuroradiology and Clinical Neuroscience Center (M.P., A. Pangalu, A.B., B.N., Z.K.), University Hospital Zurich, University of Zurich, Zurich, Switzerland.

Please address correspondence to Olivia Sobczyk, PhD, University Health Network, Toronto General Hospital, Toronto, Ontario, Canada, 200 Elizabeth St, Toronto, ON, Canada M5G 2C4, P: 647-255-1410; e-mail: olivia.sobczyk@uhn.ca

 Indicates open access to non-subscribers at www.ajnr.org

 Indicates article with online supplemental data.

<http://dx.doi.org/10.3174/ajnr.A8068>

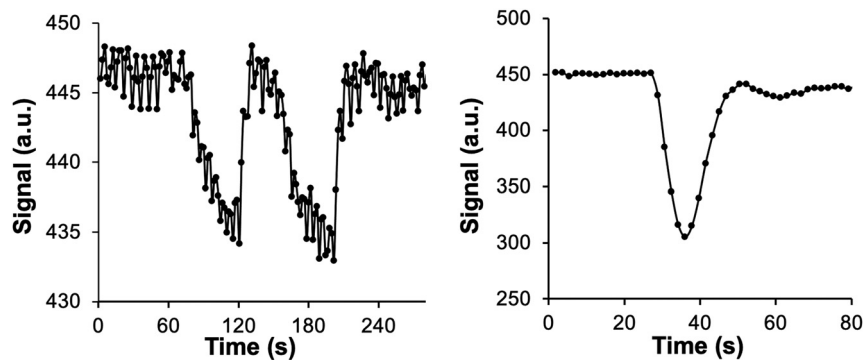


FIG 1. The 2 BOLD signal (a.u.) waveforms in a voxel over the MCA versus time in a representative participant for Thx-dOHb (A) and GBCA (B). A.u. indicates arbitrary units.

susceptibility contrast with pharmacokinetics similar to that of injected GBCA^{7,9-11} and thus lends itself to similar analysis for determining resting perfusion metrics. Indeed, in healthy volunteers, resting perfusion metrics generated with transient hypoxia-induced dOHb (THx-dOHb) have been shown to be similar in relative magnitudes and spatial distributions to those generated with GBCA.¹¹

The aim of this study was to evaluate the feasibility of examining cerebral resting perfusion metrics with THx-dOHb in patients with steno-occlusive cerebrovascular disease by comparing the metrics with those measured with GBCA. We hypothesized that resting MTT, rCBF, and rCBV obtained using GBCA and THx-dOHb would be comparable in the GM and WM of each participant and will likewise be able to distinguish flow deficits between affected and unaffected vascular territories.

MATERIALS AND METHODS

Participant and Ethics Approval

This study conformed to the standards set by the latest revision of the Declaration of Helsinki and was approved by the Ethics Committee of the Canton of Zurich (KEK Nr. 2020-02314), Zurich, Switzerland. All participants provided written, informed consent to partake in this study. We recruited 12 participants between the ages of 37 and 84 years with known large-vessel steno-occlusive disease through the neurosurgery outpatient clinic at University Hospital Zurich, Zurich, Switzerland. Ten participants completed the full experimental protocol, and 2 patients withdrew from the study during MR imaging due to discomfort during hypoxia. The ages, sex, and clinical profiles of those who completed the study and their MRAs are available in the Online Supplemental Data.

Experimental Protocol

The MR images were acquired using a 3T scanner (Magnetom Skyra VD13; Siemens) with a 32-channel head coil. The protocol consisted of a high-resolution T1-weighted structural scan followed by 2 identical blood oxygen level-dependent (BOLD) perfusion sequence scans. A high-resolution 3D T1-weighted spoiled gradient-echo volumetric sequence was acquired with the following parameters: TI = 942 ms, TR = 2400 ms, TE = 3.62 ms, flip angle = 12°, 176 slices, voxel size = 1.0 × 1.0 × 1.0 mm. The BOLD sequences consisted of a multi-slice 2D gradient-echo perfusion

sequence with the following parameters: TR = 1800 ms, TE = 30 ms, flip angle = 80°, 50 slices, voxel size = 2.5 × 2.5 × 2.5 mm. The first perfusion scan was acquired during end-tidal partial pressure of oxygen ($P_{ET}O_2$) manipulation while the second scan was acquired at normoxia following an IV injection of gadoterate meglumine (Dotarem; Guerbet).

Respiratory Protocol

All inspired gas was provided by a computerized gas blender running a prospective protocol^{12,13} to control end-tidal partial pressure of O_2 ($P_{ET}O_2$) and CO_2 independently of each other and of the pattern of breathing (RespirAct; Thornhill Medical). Patients breathed exclusively via a plastic face mask affixed to the face with skin tape (OpSite Flexifix; Smith & Nephew), making an airtight seal. The respiratory protocol consisted of a 60-second baseline $P_{ET}O_2$ of 95 mm Hg (normoxia), followed by a switch to $P_{ET}O_2$ of 40 mm Hg (hypoxia) for 60 seconds, and then a return to normoxia for 20 seconds, followed by repeat hypoxia for 60 seconds, followed by a return to normoxia (Fig 1A). Normocapnia was maintained throughout. After free breathing of room air for at least 5 minutes, gadoterate meglumine (0.1 mmol/kg) (Dotarem; Guerbet) was injected intravenously at a rate of 5 mL/s (with a baseline delay of 30 seconds before injection) followed by 30 mL of saline at a rate of 5 mL/s (Fig 1B).

Data Analysis Basics

The acquired BOLD images were volume-registered, slice-time corrected, and coregistered to the T1-weighted structural scans using Analysis of Functional Neuroimaging software (National Institutes of Health).¹⁴ The GBCA and THx-dOHb acquisitions were preprocessed in an identical manner to ensure that there was no bias toward any 1 scan. A 7-mm Gaussian spatial blur was applied to the data set. The T1-weighted structural scans were segmented into GM and WM and normalized to Montreal Neurological Institute coordinates using Statistical Parametric Mapping software (SPM8).^{15,16} The generated probability maps of GM and WM were thresholded at 70% probability. The MCA vascular territory was delineated manually on an anatomical Montreal Neurological Institute template (Online Supplemental Data). GM and WM masks were further divided into the left-hemisphere and right-hemisphere MCA.

Contrast-to-Noise Ratio and the BOLD Signal Change

The contrast-to-noise ratio (CNR) and BOLD signal change (ΔS) were calculated for GBCA and the THx-dOHb protocol, explained in additional detail by Poubanc et al.⁷ A 20-second continuous baseline signal at the beginning of each protocol was selected. A linear regression between the BOLD signal in each voxel and the average whole-brain signal (\bar{S} , see below) as the regressor was calculated with the slope determining the percentage signal change (ΔS). The whole-brain average signal (\bar{S}) was

Average measures of ΔS in percentages and the CNR calculated for GBCA and THx-dOHb for the 10 participants

	ΔS (%)		CNR	
	GM	WM	GM	WM
GBCA	25.20 (SD, 8.08)	14.78 (SD, 4.36)	11.21 (SD, 3.76)	8.17 (SD, 2.64)
THx-dOHb	5.71 (SD, 1.60)	2.87 (SD, 0.92)	6.33 (SD, 1.22)	6.41 (SD, 1.64)
P value	.002	.002	.004	.002

used as the regressor to ensure that both perfusion acquisitions could be compared, as summarized in Equation 1.

$$\text{Equation 1} \quad S = \alpha \times \bar{S} + \beta_1 \times t + \beta_2 + \varepsilon_t.$$

S is the scaled signal, α is the slope of the regression (parameter of interest), \bar{S} is the 1-dimensional time-series regressor, β_1 is the temporal linear signal drift component, β_2 is the signal baseline, and ε_t represents the residuals.

By means of the slope of the regression (α), ΔS was calculated as follows:

$$\text{Equation 2} \quad \Delta S = \alpha(\max(\bar{S}) - \min(\bar{S})).$$

$\max(\bar{S})$ and $\min(\bar{S})$ are, respectively, the minimum and maximum of the \bar{S} time-series.

The noise was determined as the SD of the residuals from the linear regression, $std(\varepsilon_t)$. As shown in Equation 3, to obtain the CNR, we calculated the ratio of a signal difference (ΔS) to the noise.

$$\text{Equation 3} \quad CNR = \frac{\Delta S}{std(\varepsilon_t)}.$$

The GM and WM average CNR and ΔS values were calculated for each participant.

Resting Perfusion Metrics

For this study, perfusion metrics for GBCA and THx-dOHb were calculated in an identical manner. A standard tracer kinetic model was used to calculate MTT and rCBV, shown in Equation 4 and explained in additional detail by Poubanc et al.⁷

$$\text{Equation 4} \quad S_{c,t} = \frac{rCBV}{MTT} \times AIF_t \otimes R_t + \beta_1 \times t + \beta_2 + \varepsilon_t.$$

We assumed a linear relationship between the perfusion signal and the concentration of GBCA and dOHb. β_1 accounts for the signal drift, β_2 accounts for the baseline, and ε_t represents the residuals. For each contrast agent, the strongest signal change over the MCA was selected as the arterial input function (AIF_t). By means of a least-squares fitting procedure, rCBV and MTT metrics were determined. To account for the stronger signal decrease seen between GBCA and THx-dOHb during bolus transit through the vasculature, a scaling factor was needed to correct for this difference to compare rCBV maps. We used the ratio between the signal generated by GBCA and THx-dOHb as the scaling factor. The higher values obtained using GBCA were divided by the scaling factor rendering equivalence between GBCA and THx-dOHb.

By means of the central volume theorem, the rCBF was then calculated as $rCBV/MTT$.¹⁷ GM CBF is approximately 50 mL/100

g/min based on reliable measurements using PET,¹⁸ therefore, all participant CBF values were scaled by 50 arbitrary units on a voxelwise basis to obtain values within a familiar normative range. Perfusion metrics were overlaid onto their respective T1-weighted structural images using Analysis of Functional

Neuroimaging software (AFNI; <http://afni.nimh.nih.gov/afni>). Resting perfusion metrics were calculated in the supratentorial cortical GM and WM for GBCA and THx-dOHb. Resting perfusion metrics in GM and WM of each cerebral hemisphere were calculated using the previously created MCA vascular territory mask.

Statistical Analysis

The CNR, ΔS , calculated perfusion metrics, and their ratios of affected and unaffected vascular territories in GM and WM were compared between GBCA and THx-dOHb using a Wilcoxon matched-pairs signed-rank test (Prism 9 software; GraphPad). Using the calculated GM and WM averages, Bland-Altman plots were generated (Prism software; GraphPad).

RESULTS

Signal Comparison

The CNR and ΔS for GM and WM are presented in the Table. The GBCA signal was 4.41 times stronger in GM ($P = .002$) and 5.15 times stronger in WM ($P = .002$) than the THx-dOHb signal. However, the GBCA CNR was only 1.77 greater in GM ($P = .004$) and 1.27 times greater in WM ($P = .002$) than the THx-dOHb CNR.

Comparison of Resting Perfusion Metrics in GM and WM

A summary of perfusion metrics between GBCA and THx-dOHb are presented in the Online Supplemental Data. A Wilcoxon matched-pairs signed-rank test did not show statistically significant differences in resting perfusion metrics between GBCA and THx-dOHb in GM or WM ($P > .05$), except for WM MTT ($P < .05$) (Online Supplemental Data). Bland-Altman plots comparing the perfusion metrics from the GBCA and THx-dOHb are presented in Fig 2. A summary of the Bland-Altman plot analysis is presented in the Online Supplemental Data. The plots have negligible constant bias or proportional bias between techniques, except for WM MTT (Online Supplemental Data).

Comparison of Resting Perfusion Metrics in Affected and Unaffected Hemispheres

Of the 10 participants who completed the study, 8 had unilateral steno-occlusive disease, while 2 had bilateral lesions. The images of those with unilateral disease were divided into affected-versus-unaffected hemispheres. Figure 3 shows the line plots of MTT, rCBF, and rCBV in the affected and unaffected hemispheres in MCA GM and WM calculated using GBCA and THx-dOHb. The trends of hemodynamic metrics between hemispheres were very similar for both contrast agents. We compared the ratios of the affected and unaffected hemispheres in GM and WM between GBCA and THx-dOHb (Online Supplemental Data). A

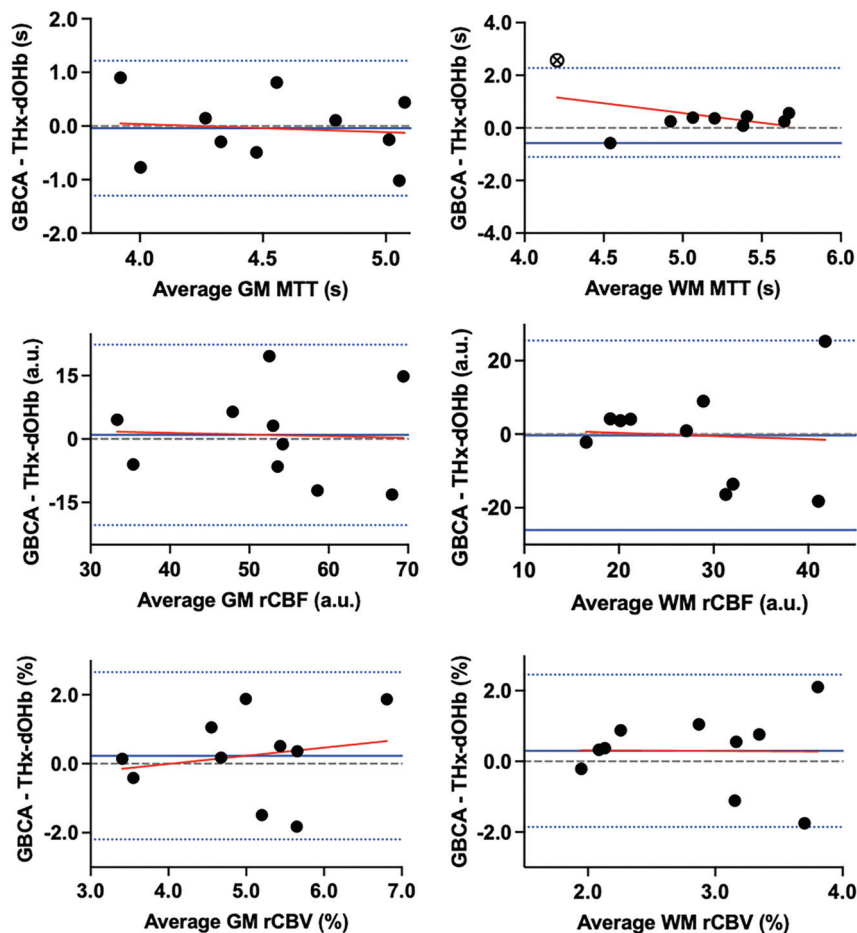


FIG 2. Bland-Altman plots comparing GBCA and THx-dOHb differences for perfusion metrics MTT, rCBF, and rCBV in GM and WM. The solid blue line depicts the mean, the dotted blue lines represent the 95% limits of agreement, and the red line represents the regression line.

Wilcoxon matched-pairs signed-rank test did not show a statistically significant difference in the ratios of affected and unaffected hemispheres between GBCA and THx-dOHb in GM or WM for all metrics ($P > .05$), except for WM rCBV (Online Supplemental Data).

Resting Perfusion Maps

Figure 4 shows perfusion maps for a representative participant (ID 1 as found in the Online Supplemental Data). This patient had a right ICA occlusion that led to a right ischemic stroke. The MTT, rCBF, and rCBV maps for the acquired images using GBCA and THx-dOHb have a high spatial similarity showing delayed MTT, slightly lower CBF, and higher CBV in the affected right hemisphere.

DISCUSSION

Main Findings

Resting cerebral perfusion metrics in patients with cerebrovascular steno-occlusive disease calculated with THx-dOHb contrast were similar to those generated with GBCA. In particular, the spatial distributions of the respective perfusion metrics MTT, rCBF, and rCBV were similar in both GM and WM. Both contrast agents were also similar, enabling the discrimination

between the affected and the unaffected hemispheres. Furthermore, the distributions of hemodynamic metrics between hemispheres were consistent with the locations of large-vessel pathology. We note that to eliminate any methodological, temporal, and disease variability, each participant was used as his or her own control. These findings, therefore, show that resting perfusion metrics obtained noninvasively with THx-dOHb can be of clinical value, particularly after considering the benefits and risks compared with GBCA.

Summary of Findings

Perfusion metrics MTT, rCBF, and rCBV were compared between GBCA and THx-dOHb in GM and WM. The perfusion metrics generated using the 2 contrast agents were not significantly different from one another, except for WM MTT. The WM MTT for THx-dOHb was significantly lower in comparison with GBCA ($P < .05$). Nevertheless, the individual participant perfusion maps are spatially very similar. Indeed, the results from the Bland-Altman plot analysis showed that the average discrepancy (constant bias) between the two agents is small for all perfusion metrics, with a narrow confidence interval, except for a constant bias for WM MTT in which the GBCA MTT is consistently greater

than THx-dOHb. Furthermore, the differences between perfusion metrics in GM or WM have no proportional bias, with the slope of the regression line not significantly different from zero. The ratio of affected and unaffected hemispheres were the same for all subjects, with each contrast except for WM rCBV.

We suggest that these findings support the continued exploration of THx-dOHb for DSC imaging as (i) there is high agreement between metrics obtained using DSC imaging with GBCA and (ii) THx-dOHb is able to discriminate between affected and unaffected hemispheres in patients with steno-occlusive disease.

Advances over Current Knowledge

This study in patients with steno-occlusive disease follows previous investigations that demonstrated the utility of THx-dOHb as a contrast agent. Poubanc et al⁷ were the first to use THx-dOHb to calculate and map voxelwise resting perfusion metrics. The investigators applied sequential gas delivery¹³ and prospective end-tidal gas targeting¹² to generate abrupt transient isocapnic reductions in oxygen, to create pharmacokinetic profiles with dOHb that are similar to those obtained from an intravascular injection of GBCA, thereby enabling a similar approach to the calculation of perfusion metrics. Subsequently Sayin et al¹¹ found that the perfusion metrics generated by the 2 contrast agents were similar when

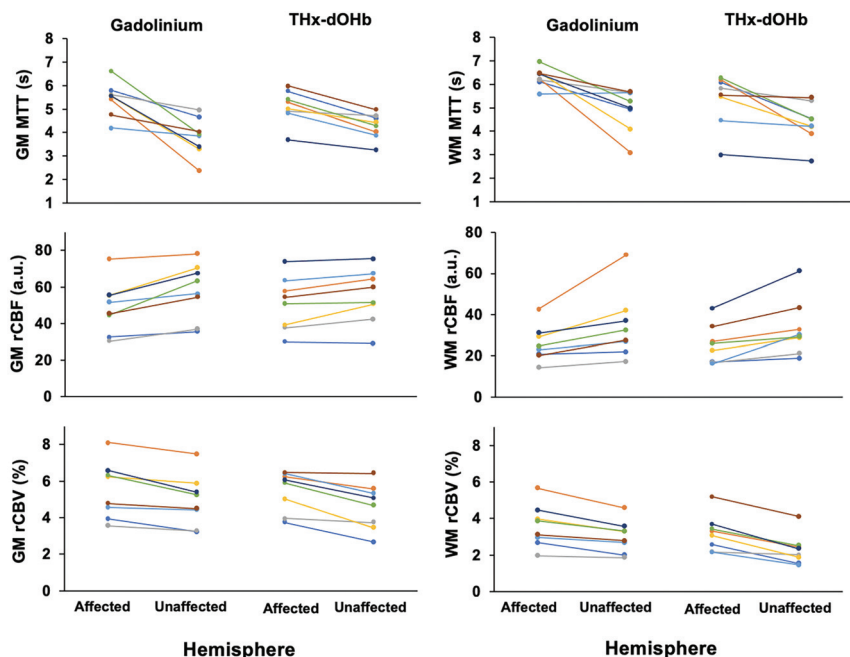


FIG 3. The affected-versus-nonaffected hemispheric perfusion metrics for GBCA and THx-dOHb for 8 participants who have unilateral steno-occlusive disease (patients 6 and 7 have bilateral disease and were excluded) in the MCA in the GM (on the right) and WM (on the left). The trends of affected-versus-unaffected hemispheres across both techniques are comparable. a.u. indicates arbitrary units.

assessed in the same healthy individuals. In this study, we extended these observations to show similarity in pattern as well as in the interpretation of perfusion metrics in patients with cerebrovascular pathology in the form of steno-occlusive disease.

THx-dOHb has several advantages over GBCAs as a contrast agent for DSC MR imaging. GBCA is an intravascular extracellular molecule. It can leak into the interstitial fluid¹⁹ in pathologic conditions when the BBB is disrupted and, therefore, requires leakage correction. By contrast, due to dOHb being contained in red cells, it remains intravascular regardless of the state of the BBB. This capacity may be a particularly useful advantage when the BBB is disrupted, provided that there is no active bleeding.²⁰ Furthermore, the analysis of the signal generated by GBCA can be affected during a second pass through the circulation, which will not occur with THx-dOHb unless there is a right-to-left cardiopulmonary shunt. On the contrary, THx-dOHb is cleared within 1 blood circulation time following pulmonary reoxygenation, enabling repeat measures as required. THx-dOHb may also be a suitable alternative contrast for patients with renal insufficiency who are at risk of nephrogenic systemic fibrosis if exposed to GBCA or at risk of worsening of renal function if exposed to iodinated contrast used for CTP.

During the past decade, there has been a drive to develop noninvasive techniques that are capable of identifying vascular dysfunction in individuals who are at risk. Arterial spin-labeling is a noninvasive MR imaging technique that provides quantitative measures of CBF. However, this technique has sensitivity to transit times and long collateral flow pathways associated with advanced cerebrovascular disease.^{21–23} Currently, the only clinical standard for assessing perfusion metrics in patients with cerebrovascular steno-

occlusive disease is DSC imaging with GBCA. However, future work comparing CBF measured via Thx-dOHb with arterial spin-labeling may be beneficial.

Bolus Profile Comparison

The stimulus profile we used in this study was chosen to be consistent with its antecedent studies. The arterial input function profile of THx-dOHb differs from that of GBCA by having 2 susceptibility oxygen desaturations (Fig 1). Due to the strong paramagnetic properties of GBCA and the rapid IV injection, GBCA causes a very sharp decrease in the BOLD signal. In contrast, the rate of dOHb formation is limited by the rate of deoxygenation in the lungs. This process is one of breath-by-breath dilution of the oxygen in the lungs, over about 5–7 breaths taking about 20 seconds. Thus, the THx-dOHb performed a double 60-second hypoxic exposure targeting partial pressure of oxygen (PO_2) of 40 mmHg to improve the CNR. Previous studies have determined that the CNR increased marginally with repeat hypoxic stimuli. Although the susceptibility profiles of GBCA and Thx-dOHb differ, the arterial input functions can be used for both agents for the calculation of the respective perfusion metrics.^{7,11} Nevertheless, further changes in the hypoxic exposure profile may be considered for implementing strategies to shorten the time to reach target hypoxia.

Limitations

The tolerance of hypoxia in humans has been well-established. In formal studies, participants maintained a PO_2 at about 50 mm Hg for >20 minutes.^{24–26} In another study, a PO_2 of 55 mm Hg was maintained for 8 hours.²⁷ Hypoxia is experienced continuously by the millions who live at high altitudes, especially those with severe lung and heart disease, and intermittently by hundreds of millions throughout the world who have multiple episodes of obstructive sleep apnea nightly. Indeed, extended periods of intermittent hypoxia have even shown benefits of preconditioning against myocardial infarction,^{28,29} heart failure,³⁰ hypertension,^{30,31} and cognitive decline.³²

There is likely a range of sensitivity to hypoxia in humans and a range of its tolerability. In this study, 2 of 12 patients did not tolerate the hypoxia and aborted their study. Both participants who aborted the study did so during the second hypoxic exposure. It is possible that the low tolerance for hypoxia was related to the severity of the perfusion limitation, though there are no indications of this effect in people with severe steno-occlusive disease living at high altitudes or with concomitant severe pulmonary disease or severe, prolonged obstructive sleep apnea.

Another limitation of THx-dOHb is the issue of CBF increase in response to hypoxia, which could confound the measurement

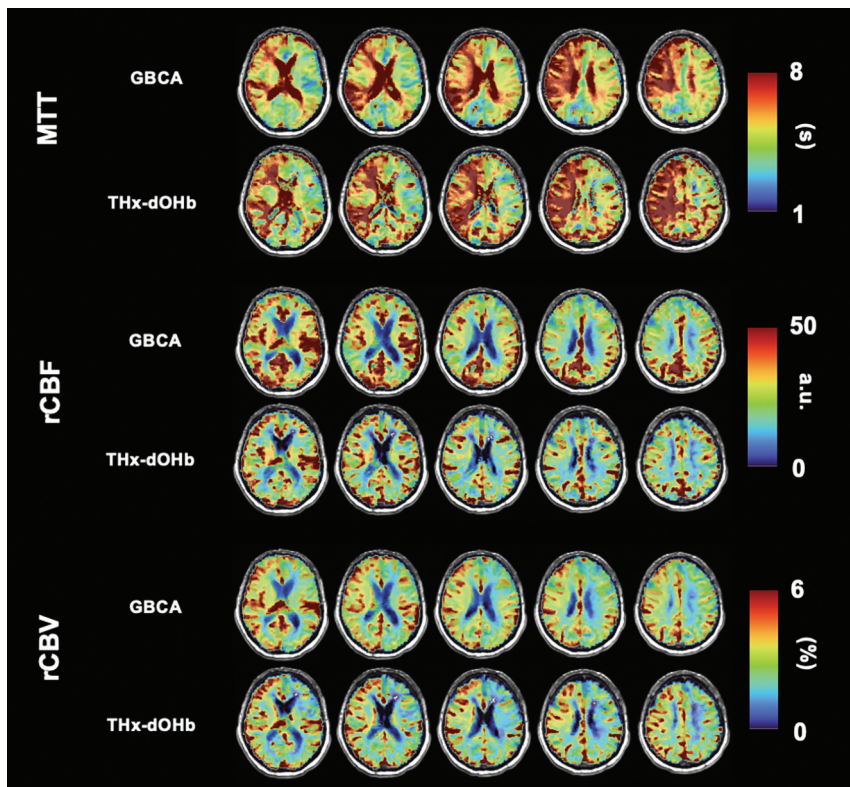


FIG 4. Perfusion maps of MTT, rCBF, and rCBV of a 71-year-old male participant (ID 1) with a right ICA occlusion comparing GBCA (A) and THx-dOHb (B). a.u. indicates arbitrary units.

of perfusion metrics. Ellingsen et al³³ had reported that a normocapnic reduction of PO₂ to 65 mm Hg resulted in an increase in carotid artery blood flow velocity over a period of about 10 minutes with a halftime of about 4 minutes. More recently, Harris et al²⁴ used pulsed arterial spin-labeling to measure the delay and time constant of a CBF increase in response to acute hypoxia. They found a delay to onset of flow change of about 3 minutes with a time constant of about 4.5 minutes. The duration of our hypoxic stimuli was only 60 seconds, repeated twice. However, the precise kinetics of CBF responses to acute severe hypoxia have not been rigorously documented.³⁴ If acute hyperemic responses do occur, reducing the extent of hypoxia or shortening the hypoxic interval may be feasible. These measures would also increase the tolerability of hypoxia.^{7,35,36} A further limitation may occur in areas of misery perfusion in which blood flow is low and the oxygen extraction fraction is high, resulting in a high baseline concentration of dOHb. With the initiation of THx-dOHb, the arterial oxygen delivery is further reduced, resulting in an exaggerated fall in the BOLD signal, perhaps marking the area of misery perfusion.

The presence of steno-occlusive disease or cerebral ischemia may itself result in dispersion of the bolus of contrast³⁷ and difficulty in accurately applying the input function. There are numerous ways to analyze perfusion data including, but not limited to, adopting a mono-/biexponential model from pharmacokinetics,³⁸ or using a vascular model³⁹ or a singular value decomposition.⁴⁰ However, these deconvolution techniques do not account for dispersion. For that, a complex model for the vasculature is required.⁴¹ When there is no correction for contrast dispersion, caution should

be used in interpreting the calculated MTT, rCBF, and rCBV metrics from either contrast. Similarly, if such peripheral late dispersion does exist, the deconvolution model would be equally offset with both GBCA and THx-dOHb profiles.

CONCLUSIONS

Cerebral perfusion metrics, including MTT, rCBF, and rCBV, using the novel contrast agent THx-dOHb show high spatial and scalar congruence with those generated by GBCA in subjects with known cerebrovascular steno-occlusive disease. In selected patients, THx-dOHb has the advantages of being needle-free and suitable for unlimited repeat examinations. These findings support the continued investigation of THx-dOHb as a noninvasive endogenous contrast agent to obtain cerebral perfusion metrics.

ACKNOWLEDGMENTS

All the authors thank University Hospital Zurich MR technologist Maria Sarioglou for all her help in acquiring the MR imaging data.

Disclosure forms provided by the authors are available with the full text and PDF of this article at www.ajnr.org.

REFERENCES

- Calamante F, Ganesan V, Kirkham FJ, et al. **MR perfusion imaging in moyamoya syndrome.** *Stroke* 2001;32:2810–16 [CrossRef Medline](#)
- Kanal E. **Gadolinium based contrast agents (GBCA): safety overview after 3 decades of clinical experience.** *Magn Reson Imaging* 2016;34:1341–45 [CrossRef Medline](#)
- Gulani V, Calamante F, Shellock FG, et al; International Society for Magnetic Resonance in Medicine. **Gadolinium deposition in the brain: summary of evidence and recommendations.** *Lancet Neurol* 2017;16:564–70 [CrossRef Medline](#)
- Cheng HL. **Investigation and optimization of parameter accuracy in dynamic contrast-enhanced MRI.** *J Magn Reson Imaging* 2008;28:736–43 [CrossRef Medline](#)
- Calamante F, Connelly A, van Osch MJ. **Nonlinear ΔR effects in perfusion quantification using bolus-tracking MRI.** *Magn Reson Med* 2009;61:486–92 [CrossRef Medline](#)
- Pauling L, Coryell CD. **The magnetic properties and structure of hemoglobin, oxyhemoglobin and carbonmonoxyhemoglobin.** *Proc Natl Acad Sci U S A* 1936;22:210–16 [CrossRef Medline](#)
- Poublanc J, Sobczyk O, Shafi R, et al. **Perfusion MRI using endogenous deoxyhemoglobin as a contrast agent: preliminary data.** *Magn Reson Med* 2021;86:3012–21 [CrossRef Medline](#)
- Vu C, Chai Y, Coloigner J, et al. **Quantitative perfusion mapping with induced transient hypoxia using BOLD MRI.** *Magn Reson Med* 2021;85:168–81 [CrossRef Medline](#)
- Bhogal AA, Sayin ES, Poublanc J, et al. **Quantifying cerebral blood arrival times using hypoxia-mediated arterial BOLD contrast.** *Neuroimage* 2022;261:119523 [CrossRef Medline](#)
- Schulman JB, Sayin ES, Manalac A, et al. **DSC MRI in the human brain using deoxyhemoglobin and gadolinium: simulations and**

- validations at 3T. *Front Neuroimaging* 2023;2:1048652 [CrossRef Medline](#)
11. Sayin ES, Schulman J, Poubanc J, et al. Investigations of hypoxia-induced deoxyhemoglobin as a contrast agent for cerebral perfusion imaging. *Hum Brain Mapp* 2023;44:1019–29 [CrossRef Medline](#)
12. Slessarev M, Han J, Mardimae A, et al. Prospective targeting and control of end-tidal CO₂ and O₂ concentrations. *J Physiol* 2007;581:1207–19 [CrossRef Medline](#)
13. Fisher JA, Iscoe S, Duffin J. Sequential gas delivery provides precise control of alveolar gas exchange. *Respir Physiol Neurobiol* 2016;225:60–69 [CrossRef Medline](#)
14. Cox RW. AFNI: software for analysis and visualization of functional magnetic resonance neuroimages. *Comput Biomed Res* 1996;29:162–73 [CrossRef Medline](#)
15. Ashburner J, Friston K. Multimodal image coregistration and partitioning—a unified framework. *Neuroimage* 1997;6:209–17 [CrossRef Medline](#)
16. Ashburner J, Friston KJ. Unified segmentation. *Neuroimage* 2005;26:839–51 [CrossRef Medline](#)
17. Ostergaard L. Principles of cerebral perfusion imaging by bolus tracking. *Magn Reson Imaging* 2005;22:710–17 [CrossRef](#)
18. Fantini S, Sassaroli A, Tgavalekos KT, et al. Cerebral blood flow and autoregulation: current measurement techniques and prospects for noninvasive optical methods. *Neurophotonics* 2016;3:031411 [CrossRef Medline](#)
19. Quarles CC, Bell LC, Stokes AM. Imaging vascular and hemodynamic features of the brain using dynamic susceptibility contrast and dynamic contrast enhanced MRI. *Neuroimage* 2019;187:32–55 [CrossRef Medline](#)
20. Kanda T, Ishii K, Kawaguchi H, et al. High signal intensity in the dentate nucleus and globus pallidus on unenhanced T1-weighted MR images: relationship with increasing cumulative dose of a gadolinium-based contrast material. *Radiology* 2014;270:834–41 [CrossRef Medline](#)
21. Buxton RB, Frank LR, Wong EC, et al. A general kinetic model for quantitative perfusion imaging with arterial spin labeling. *Magn Reson Med* 1998;40:383–96 [CrossRef Medline](#)
22. Mandell DM, Han JS, Poubanc J, et al. Selective reduction of blood flow to white matter during hypercapnia corresponds with leukoariosis. *Stroke* 2008;39:1993–98 [CrossRef Medline](#)
23. van Gelderen P, de Zwart JA, Duyn JH. Pitfalls of MRI measurement of white matter perfusion based on arterial spin labeling. *Magn Reson Med* 2008;59:788–95 [CrossRef Medline](#)
24. Harris AD, Murphy K, Diaz CM, et al. Cerebral blood flow response to acute hypoxic hypoxia. *NMR Biomed* 2013;26:1844–52 [CrossRef Medline](#)
25. Mahamed S, Duffin J. Repeated hypoxic exposures change respiratory chemoreflex control in humans. *J Physiol* 2001;534:595–603 [CrossRef Medline](#)
26. Mahamed S, Cunningham DA, Duffin J. Changes in respiratory control after three hours of isocapnic hypoxia in humans. *J Physiol* 2003;547:271–81 [CrossRef Medline](#)
27. Ren X, Dorrington KL, Robbins PA. Respiratory control in humans after 8 h of lowered arterial PO₂, hemodilution, or carboxyhemoglobinemia. *J Appl Physiol* (1985) 2001;90:1189–95 [CrossRef Medline](#)
28. Nakada Y, Canseco DC, Thet S, et al. Hypoxia induces heart regeneration in adult mice. *Nature* 2017;541:222–27 [CrossRef Medline](#)
29. Almendros I, Wang Y, Gozal D. The polymorphic and contradictory aspects of intermittent hypoxia. *Am J Physiol Lung Cell Mol Physiol* 2014;307:L129–40 [CrossRef Medline](#)
30. Serebrovskaya TV, Manukhina EB, Smith ML, et al. Intermittent hypoxia: cause of or therapy for systemic hypertension? *Exp Biol Med (Maywood)* 2008;233:627–50 [CrossRef Medline](#)
31. Ghofrani HA, Voswinckel R, Reichenberger F, et al. Hypoxia- and non-hypoxia-related pulmonary hypertension: established and new therapies. *Cardiovasc Res* 2006;72:30–40 [CrossRef Medline](#)
32. Navarrete-Opazo A, Mitchell GS. Therapeutic potential of intermittent hypoxia: a matter of dose. *Am J Physiol Regul Integr Comp Physiol* 2014;307:R1181–97 [CrossRef Medline](#)
33. Ellingsen I, Hauge A, Nicolaysen G, et al. Changes in human cerebral blood flow due to step changes in PAO₂ and PACO₂. *Acta Physiol Scand* 1987;129:157–63 [CrossRef Medline](#)
34. Mardimae A, Balaban DY, Machina MA, et al. The interaction of carbon dioxide and hypoxia in the control of cerebral blood flow. *Pflugers Arch* 2012;464:345–51 [CrossRef](#)
35. Balaban DY, Duffin J, Preiss D, et al. The in-vivo oxyhaemoglobin dissociation curve at sea level and high altitude. *Respir Physiol Neurobiol* 2013;186:45–52 [CrossRef Medline](#)
36. Battisti-Charbonney A, Fisher JA, Duffin J. Respiratory, cerebrovascular and cardiovascular responses to isocapnic hypoxia. *Respir Physiol Neurobiol* 2011;179:259–68 [CrossRef Medline](#)
37. Calamante F, Yim PJ, Cebral JR. Estimation of bolus dispersion effects in perfusion MRI using image-based computational fluid dynamics. *Neuroimage* 2003;19:341–53 [CrossRef Medline](#)
38. Lassen NA, Andersen AR, Friberg L, et al. The retention of [99mTc]-d,l-HM-PAO in the human brain after intracarotid bolus injection: a kinetic analysis. *J Cereb Blood Flow Metab* 1988;8:S13–22 [CrossRef Medline](#)
39. Mouridsen K, Friston K, Hjort N, et al. Bayesian estimation of cerebral perfusion using a physiological model of microvasculature. *Neuroimage* 2006;33:570–79 [CrossRef Medline](#)
40. Ostergaard L, Weisskoff RM, Chesler DA, et al. High resolution measurement of cerebral blood flow using intravascular tracer bolus passages, Part I: mathematical approach and statistical analysis. *Magn Reson Med* 1996;36:715–25 [CrossRef Medline](#)
41. Ostergaard L, Chesler DA, Weisskoff RM, et al. Modeling cerebral blood flow and flow heterogeneity from magnetic resonance residue data. *J Cereb Blood Flow Metab* 1999;19:690–99 [CrossRef Medline](#)